Viscoplastic Effects Occurring in Impacts of Aluminum and Steel Bodies and Their Influence on the Coefficient of Restitution

Robert Seifried[1]
Institute of Engineering and Computational Mechanics,
University of Stuttgart,
Pfaffenwaldring 9, 70569 Stuttgart, Germany
e-mail: seifried@itm.uni-stuttgart.de

Hirofumi Minamoto
Department of Mechanical Engineering,
Toyohashi University of Technology,
1-1 Tempaku-cho Toyohashi, Aichi 441-8580, Japan
e-mail: minamoto@mech.tut.ac.jp

Peter Eberhard
Institute of Engineering and Computational Mechanics,
University of Stuttgart,
Pfaffenwaldring 9, 70569 Stuttgart, Germany
e-mail: eberhard@itm.uni-stuttgart.de

Generally speaking, impacts are events of very short duration and a common problem in machine dynamics. During impact, kinetic energy is lost due to plastic deformation near the contact area and excitation of waves. Macromechanically, these kinetic energy losses are often summarized and expressed by a coefficient of restitution, which is then used for impact treatment in the analysis of the overall motion of machines. Traditionally, the coefficient of restitution has to be roughly estimated or measured by experiments. However, more recently finite element (FE) simulations have been used for its evaluation. Thereby, the micromechanical plastic effects and wave propagation effects must be understood in detail and included in the simulations. The plastic flow, and thus the yield stress of a material, might be independent or dependent of the strain-rate. The first material type is called elastic-plastic and the second type is called elastic-viscoplastic. In this paper, the influence of viscoplasticity of aluminum and steel on the impact process and the consequences for the coefficient of restitution is analyzed. Therefore, longitudinal impacts of an elastic, hardened steel sphere on aluminum AL6060 rods and steel S235 rods are investigated numerically and experimentally. The dynamic material behavior of the specimens is evaluated by split Hopkinson pressure bar tests and a Perzyna-like material model is identified. Then, FE impact simulations and impact experiments with laser-doppler-vibrometers are performed. From these investigations it is shown that strain-rate effects of the yield stress are extremely small for impacts on aluminum but are significant in impacts on steel. In addition, it is demonstrated that it is possible to evaluate for both impact systems the coefficient of restitution numerically, whereas for the aluminum body a simple elastic-plastic material model is sufficient. However, for the steel body an elastic-viscoplastic material model must be included. [DOI: 10.1115/1.4000912]

Keywords: impact, coefficient of restitution, aluminum, steel, finite elements, experiment, strain-rate effect, plasticity

1 Introduction

Impacts are a common problem in many machine dynamic applications, e.g., gear trains, electromagnetic valves, or hammer drills. Impacts are events of very short duration during which kinetic energy of the rigid body motion can be lost due to inelastic deformation of the contact area and excitation of waves in the bodies [1–3]. Even in low velocity impacts typically found in machine dynamics, these two effects often occur simultaneously. Macromechanically, these kinetic energy losses are often summarized and expressed by a coefficient of restitution. There are mainly three definitions of the coefficient of restitution, namely, kinematic, kinetic, and energetic definition of the coefficient of restitution [4]. In this paper, the kinetic definition of the coefficient of restitution is chosen, which is defined as the ratio of impulse during compression and restitution phase. The coefficient of restitution forms the basis for impact treatment by continuous compliance models [5] or instantaneous impact models [6]. These are most useful in the analysis of the overall motion in machine dynamics.

The coefficient of restitution must be estimated from experience or measured by costly experiments. Several experimental results for the coefficient of restitution are available in literature, see, e.g., Refs. [7–9]. More recently, finite element (FE) simulations have been used to numerically evaluate the coefficient of restitution [10–12]. In order to have sound results, the micromechanical plastic effects and wave propagation effects need to be understood in detail and included in the simulations.

While for some materials the plastic flow is independent of the strain-rate, other materials show a significant increase of the yield stress with the strain-rate [13]. The first type of material behavior is referred to as elastic-plastic material behavior, whereas the second type is referred to as elastic-viscoplastic material behavior. Material tests available in literature, see, e.g., Ref. [13], show for aluminum alloys only little influence of the strain-rate, conversely steels often have a distinct elastic-viscoplastic material behavior. For impacts of aluminum bodies assuming elastic-plastic material behavior, there are several numerical results available in literature, e.g., Refs. [10,11], and validated experimentally [2,3,12,14]. However, in machine dynamics the effects of strain-rate sensitivity of the yield stress on impact process and its influence on the coefficient of restitution has not yet been investigated in great detail. Very few numerical and experimental results for machine dynamics impacts of steel bodies with elastic-viscoplastic material behavior are available [15,16].

In this paper, the focus is on a detailed analysis of the influence of viscoplasticity of aluminum and steel on the impact process and the consequences for the coefficient of restitution. Aluminum AL6060 and steel S235 are chosen as experimental materials.

[1]Corresponding author.

Contributed by the Applied Mechanics Division of ASME for publication in the JOURNAL OF APPLIED MECHANICS. Manuscript received February 20, 2009; final manuscript received November 20, 2009; published online April 9, 2010. Assoc. Editor: Vikram Deshpande.

Table 1 Basic material data of the impact systems

	Material	Young's modulus (GPa)	Possion ratio	Density (kg/m^3)
Sphere	100Cr6	210	0.3	7780
Rod	AL6060	67.7	0.33	2702
Rod	S235	208	0.3	7800

First, the quasi-static material behavior is measured by quasi-static compression tests. The behavior under various strain-rates is measured by Split Hopkinson pressure bar tests and from these measurements a Perzyna-like elastic-viscoplastic material model is identified. Then, longitudinal impacts of an elastic, hardened steel sphere on aluminum AL6060 rods and steel S235 rods are investigated numerically and experimentally. The velocity range 0.05–3.5 m/s is investigated, which are typical velocities in machine dynamics impacts. In the numerical impact investigation nonlinear FE models are used, considering elastic, elastic-plastic, and elastic-viscoplastic material behavior. In the experimental impact investigation laser-doppler-vibrometers (LDVs) are used to measure the velocities of the bodies during impact. From these investigations it is shown that the strain-rate effects of the yield stress are negligible for impacts on the aluminum but significant for the steel bodies. In addition, it is demonstrated that for both impact systems it is possible to evaluate accurately the coefficient of restitution numerically. Therefore, in the impact on the aluminum body a simple elastic-plastic material model is sufficient while for the impact on the steel body an elastic-viscoplastic material model must be included.

2 Impact System and Material Properties

In this paper, the longitudinal impact of a sphere on a resting rod along its longitudinal axis is considered as a test example. The sphere is made of material 100Cr6 and has a radius of 15 mm. Two types of rods are used: aluminum rods made of AL6060 and steel rods made of S235, which is the Euronorm equivalent of A283C. Both types of rods have circular cross section with radius of 10 mm and a length of 1000 mm. The basic material data of the impacting bodies are summarized in Table 1.

The steel sphere originates from a ball-bearing, is hardened and thus is considered as being elastic. During impact plastic deformation occurs only in the rods. The static stress-strain curves of both specimens are obtained from quasi-static compression tests. The measured yield stress σ_y of AL6060 is 205 MPa and of S235 is 230 MPa. Figure 1 shows the piecewise linear approximation of the measured static stress-strain curves, which are then used in the FE simulations.

As described in Ref. [13], the plastic flow of some materials might depend on the strain-rate $\dot{\epsilon}=d\epsilon/dt$. This so-called elastic-viscoplastic behavior is a material property, which is independent of the body geometry. For the evaluation of the aluminum and steel material behavior under high strain-rates split Hopkinson pressure bar tests are performed. A detailed review of high strain-rate material testing methods and especially the split Hopkinson pressure bar test are given in Refs. [17,18]. Figure 2 shows for aluminum AL6060 and steel S235 the measured stress-strain curves for strain-rates between 100 l/s and 6000 l/s, which are measured during plastic deformation of the specimens. Also the quasi-static stress-strain curves are added. The plots indicate that the aluminum used does not show any strain-rate effects for low strain-rates and only a modest increase of the yield stress for higher strain-rates. For example, for strain-rates over 1000 l/s the aluminum specimens show only an increase of the yield stress by a factor of approximately 1.5. In contrast, even in low strain-rates the steel specimens show a significant increase of the yield stress and the stress-strain curve. For strain-rates over 1000 l/s the steel specimens show an increase by a factor of over 4. This clearly demonstrates that the steel specimens have a strong strain-rate dependency.

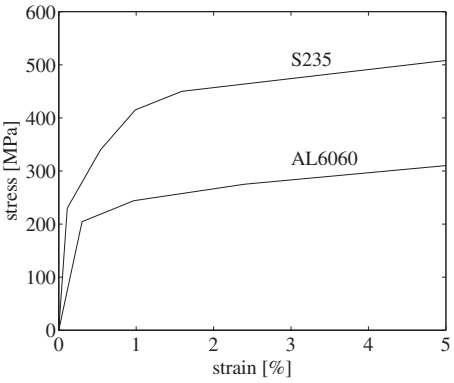

Fig. 1 Approximation of static stress-strain curves

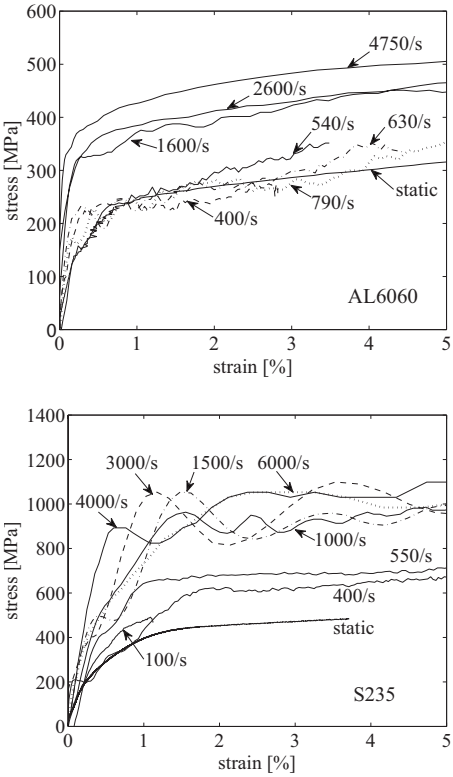

Fig. 2 Measured stress-strain curves for AL6060 and S235

For the mathematical description of this viscoplastic material behavior a Perzyna type material model [19,20] can be used. In the used Perzyna model the dynamic yield stress σ_d is expressed as

$$\sigma_d = \beta\sigma_y \quad \text{with} \quad \beta = \left[1 + \left(\frac{\dot{\epsilon}^{pl}}{\gamma}\right)\right]^m \tag{1}$$

In this model, σ_y is the quasi-static yield stress and β is a scaling factor, which is a function of effective plastic strain-rate $\dot{\epsilon}^{pl}$, the material viscosity parameter γ, and the strain-rate hardening parameter m. Thus, this scaling factor expresses the increase of dynamic yield stress with the plastic strain-rate. Generally, the linear strain tensor $\boldsymbol{\epsilon}$ can be decomposed into an elastic and plastic part such that $\boldsymbol{\epsilon}=\boldsymbol{\epsilon}^e+\boldsymbol{\epsilon}^{pl}$. The effective plastic strain-rate $\dot{\epsilon}^{pl}$ is then a scalar measure of the plastic strain-rate $\dot{\boldsymbol{\epsilon}}^{pl}=d\boldsymbol{\epsilon}^{pl}/dt$ at a point of the body. In metals plastic deformation is assumed to be incom-

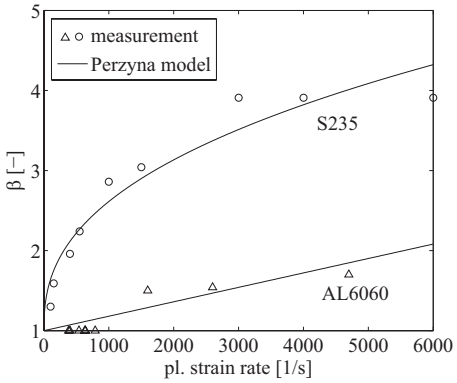

Fig. 3 Strain-rate scaling factor β

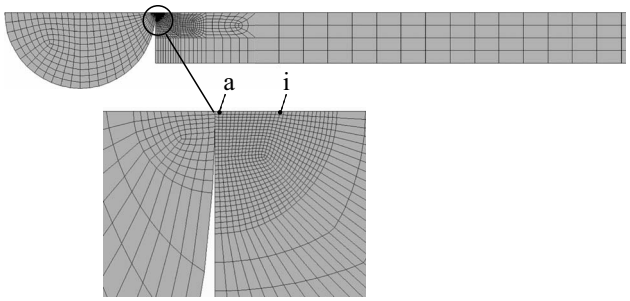

Fig. 4 Finite element model of sphere to rod impact

pressible and thus the deviatoric strain tensor $\boldsymbol{\epsilon}'$ is often used instead of $\boldsymbol{\epsilon}$ [20–22]. In the case of uniaxial loading, as it occurs in the Hopkinson Pressure Bar test, $\dot{\epsilon}^{pl}$ is equivalent to the measured strain-rates presented in Fig. 2.

The parameters γ and m of the Perzyna model have to be determined by a parameter identification from the measurements with the Hopkinson pressure bar presented in Fig. 2. Therefore, for each measurement the dynamic yield stress σ_d is identified and the scaling factors $\beta=\sigma_d/\sigma_y$ are computed. These are given in Fig. 3. Then, the two parameters γ, m are found by minimizing the squared error between the scaling factors of the measurements and the Perzyna model. For this parameter identification the MATLAB optimization toolbox is used. The quasi-static yield stress and the identified parameters γ,m of the Perzyna model are summarized in Table 2. In Fig. 3 the corresponding curves from the Perzyna model are added. This shows the good agreement of the measurement and identified Perzyna model. It should be noted that the identified elastic-viscoplastic model for the aluminum is very close to a linear behavior.

3 Simulation Model

For a detailed numerical analysis of the considered impact systems, nonlinear material behavior as well as elastodynamic wave effects must be included. However, it should be noted that due to the low velocities only small deformations occur. Thus, the computational impact analysis is carried out by using nonlinear FE method using the FE program ANSYS [23]. The theoretical background and detailed information of FE contact can be found in Refs. [24–26] and the inclusion of nonlinear materials is described in Refs. [20–22]. Detailed descriptions of various FE models of impact problems can be found in Refs. [10,11,27]. For an accurate evaluation of the impact process with FE great attention has to be placed on the choice of simulation parameters, such as spatial discretization and time step size. According to measurements, the impact problems investigated in this paper show wave phenomena up to 50–100 kHz. Following Ref. [27], the correct evaluation of these high-frequency phenomena requires a time step size of 10^{-6} s and an overall small element size of 3 mm. However, the contact radius is much smaller, about 1–2 mm. Thus, a very fine discretization of the contact region is required in order to represent the contact and the resulting stresses accurately. For the simulation a two-dimensional rotational symmetric model is used. Figure 4 shows the FE mesh near the contact region, including the sphere and the first 100 mm of the rod. In Fig. 4 also the mesh refinements near the contact area are clearly seen. The points indicated with *a* and *i* in the enlargement of the figure are located on the rotation axis of the rod and are later used for a detailed investigation of the micromechanical behavior during impact. The two discretized bodies are connected by node-to-element contact elements (element type *Targe* 169/*Contal* 175) and a Lagrange contact formulation is used in the simulation.

Table 2 Yield stress and Perzyna parameters

	σ_y (MPa)	γ	m
AL6060	205	5548	1
S235	230	305	0.403

For the discretization of the sphere and rod two-dimensional rotational symmetric elements (element type *Plane* 182) are used. These elements are capable of handling elastic, elastic-plastic as well as elastic-viscoplastic material behavior. In the elastic-plastic model post-yield isotropic hardening is achieved by using the piecewise linear static stress-strain curves, which are shown in Fig. 1. In the elastic-viscoplastic simulation the Perzyna model given by Eq. (1) is used with the parameters summarized in Table 2. Thereby, the Perzyna model is also combined with isotropic hardening using the static stress-strain curves shown in Fig. 1. Thus increasing strain-rates result not only in an increase of the yield stress but also result in the same way in an increase of the post-yield stress-strain curve. Compared with elastic-plastic material behavior the main difference in the numerical implementation of elastic-viscoplastic material is the rate-dependency of the constitutive material equation. The constitutive equation must be fulfilled at each element. Since the Gaussian integration is employed for each element, the effective plastic strain-rates are evaluated internally at the Gaussian integration points. Detailed descriptions of the numerical implementation of elastic-plastic and elastic-viscoplastic materials are given in Refs. [20–23].

In the Perzyna model given by Eq. (1), the effective plastic strain-rate $\dot{\epsilon}^{pl}$ is required, which is a scalar measure of the plastic strain-rate. With the effective plastic strain-increment $\Delta\epsilon'^{pl}$ in one time increment Δt the effective plastic strain-rate can be written as $\dot{\epsilon}^{pl}=\Delta\epsilon'^{pl}/\Delta t$. As shown in Ref. [21], the effective plastic strain-increment computes as

$$\Delta\epsilon'^{pl}=\sqrt{\frac{2}{3}\Delta\epsilon'^{pl}\cdot\cdot\,\Delta\epsilon'^{pl}} \tag{2}$$

where $\Delta\epsilon'^{pl}$ is the increment of the deviatoric plastic strain tensor computed in the time increment Δt. The accumulation of the increments of the effective plastic strain yields the effective plastic strain, which is a monotonically increasing scalar function describing the amount of permanent plastic strain.

4 Impact Experiment Setup

The used experimental setup for impact investigation is shown in Fig. 5 and is described in detail in Ref. [14]. The sphere and rod are suspended in a pendulum-like manner by thin kevlar wires in a frame. The steel sphere is released by a magnet from a predefined height, and it impacts the resting rod in longitudinal direction. It should be noted that each impact occurs on an undamaged surface of the rod, i.e., there is no deformation from previous

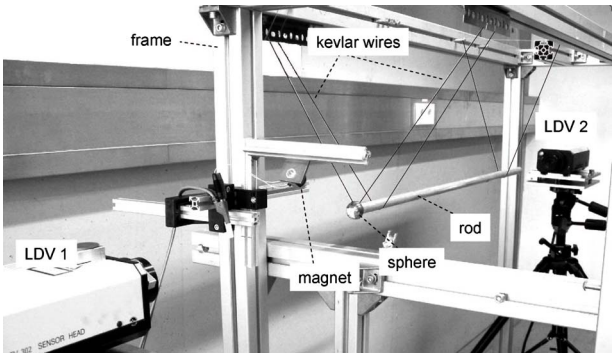

Fig. 5 Experimental setup of sphere to rod impact

impacts. Repeated impacts on previously deformed surfaces are discussed in Ref. [12]. Two LDVs of type OFV-3000/OFV-302 made by Polytec GmbH [28] are placed on opposite sides of the impact systems along the impact line. The LDVs are used to simultaneously measure the velocities and displacements of both impacting bodies. During impact, the motion of the bodies can be considered as free horizontal motion. The very high accuracy of the measurement equipment and the high quality of the experimental setup as well as the ease of reproducibility of the experiments is proven in Ref. [14].

The impact force is a very useful quantity to investigate the micromechanical processes during impact. For impacts on long rods, the impact force can be determined from measurements of the wave propagation in the rod [29]. During impact, kinetic energy is transformed into strain-energy, which propagates as a wave away from the contact region. The investigated rods are long enough such that the contact ends before the reflected wave returns to the struck end. After the wave passes a certain point of the rod, this point remains at rest until the wave passes through it again. Based on the wave equation for a rod [30], the impact force can be determined from the LDV velocity measurement v_{fe} at the free end of the rod as

$$F_v = \frac{AEv_{fe}}{2c} \quad \text{with} \quad c = \sqrt{\frac{E}{\rho}} \tag{3}$$

Thereby, c is the wave speed in the rod and A, E, and ρ denote the cross section, Young's modulus, and density of the rod, respectively. The accuracy and reliability of this impact force measurement technique is verified by comparison with impact force measurements using strain gauges and presented in Ref. [2].

For the evaluation of the overall impact behavior the kinetic coefficient of restitution is determined from the LDV velocity measurements. The kinetic coefficient of restitution is defined as the ratio of impulse during the compression and restitution phases of the impact, see Ref. [4]. It should be noted that for the investigated central impacts the definition of the kinetic coefficient of restitution is equivalent to kinematic and energetic definitions of the coefficient of restitution. Since the rods are initially at rest, the kinetic coefficient of restitution can be evaluated experimentally just from the measurements of the initial velocity v_0 of the sphere, its change of velocity Δv due to impact and the mass m_s and m_r of sphere and rod, respectively. Consequently for the sphere, the impulse produced by impact follows as $\Delta p = m_s \Delta v$. Based on the assumption for rigid body impacts the impact duration is infinitesimal and all forces except the impact force are negligible. Following Ref. [2] and establishing the linear momentum balance in the central impact line of two colliding bodies during the compression and restitution phases, the coefficient of restitution is computed as

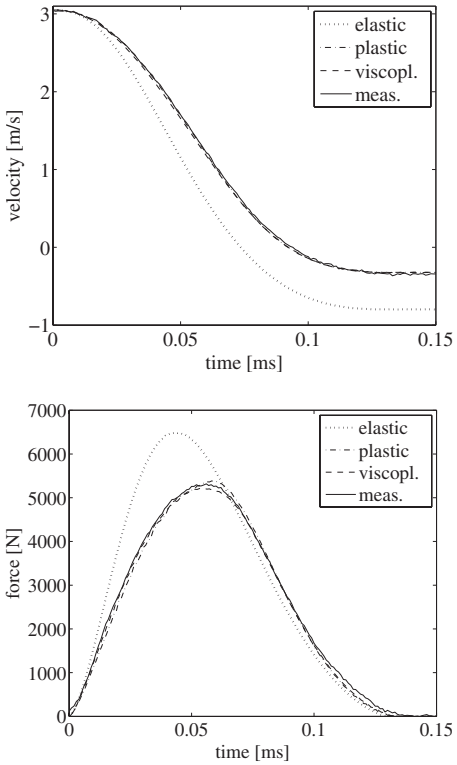

Fig. 6 Sphere velocity and impact force for impact with $v_0 = 3.05$ m/s on the aluminum rod

$$e = \frac{(m_r + m_s)\Delta v}{m_r v_0} - 1 \tag{4}$$

The same procedure is also applied to the numerical evaluation of the coefficient of restitution from the simulation results.

5 Numerical and Experimental Studies

For the analysis of the impacts, numerical simulations are performed using elastic, elastic-plastic and elastic-viscoplastic material models for both, aluminum and steel. These simulation results are then compared with the impact measurements. At first, impacts on the aluminum rods are analyzed followed by impacts on the steel rods.

Figure 6 shows a longitudinal impact with $v_0 = 3.05$ m/s on the aluminum rod, presenting the measured and simulated sphere velocity during impact and the impact force. The simulated sphere velocity is taken from the results of the dynamic FE simulation for the center of the sphere. The simulated impact force is calculated as sum of the contact forces of all contact elements. Note the short impact duration of less than 0.15 ms. It is obvious that the simulation with elastic material deviates strongly from the measurements, which shows the strong influence of plastic deformation, which may not be neglected. For the aluminum rod, the simulations with elastic-plastic and elastic-viscoplastic material models yield nearly identical results and agree very well with the measurements.

The temporal evolution of the rate of plastic deformation at various points along the axis of the rod is presented in Fig. 7. The given results are taken from the simulations with elastic-viscoplastic material behavior. Since ANSYS does not provide a direct output of the effective plastic strain-rate, the strain-rate must be computed in a post-processing step by numerical differentiation of the effective plastic strain results. It should be noted, that in the course of the numerical solution the effective strain-rates are computed at the integration points of the elements while here they are given at the nodes of the elements. The first point *a*

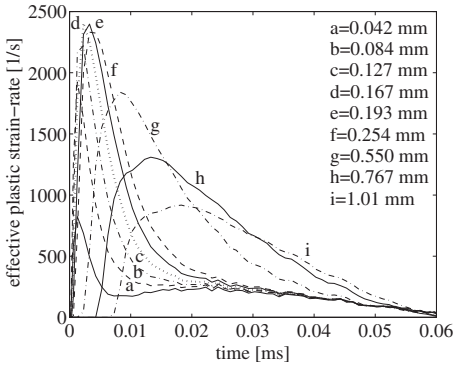

Fig. 7 Effective plastic strain-rate along the axis of the aluminum rod for impact with v_0=3.05 m/s

is located 0.042 mm and the last point *i* is located 1.01 mm away from the initial point of impact. These points are also indicated in Fig. 4 of the FE mesh. This analyzed area is the region where the main part of the plastic deformation is concentrated. The maximal effective plastic strain that occurs in this impact is 3.6%. From this plot, it is seen that for the points very close to the initial impact point very high plastic strain-rates of up to 2500 l/s occur. However, due to the very modest increase of the yield stress of the aluminum with the strain-rate, it is concluded that these high strain-rates do not influence significantly the impact behavior.

Since these results show no measurable influence of strain-rate effects in the impact on the aluminum rod, the use of an elastic-plastic material model is justified. This is in accordance with previously published comparisons of measurement and FE simulations using elastic-plastic material behavior for impacts on various aluminum bodies [3,12,14]. Finally, it is noted that for the impacts on the aluminum rod the discussed results are representative for the whole investigated velocity range.

For the impact with v_0=3.05 m/s on the steel rod, the measured and simulated sphere velocity and impact force are presented in Fig. 8. Similar to the aluminum rod, the simulation with elastic material deviates strongly from the measurements and shows again the strong influence of plastic deformation. However, in contrast to aluminum, for the steel rod the simulations with elastic-plastic and elastic-viscoplastic material models differ significantly. The simulation with the elastic-viscoplastic material model shows a higher rebound velocity, a higher maximal impact force and slightly shorter impact duration than the simulation with elastic-plastic material behavior. The simulation results from the elastic-viscoplastic material lie between the results from simulations with elastic material and elastic-plastic material. This is due to the increase of the yield stress with the strain-rate for the elastic-viscoplastic material, which yields less plastic deformation than the elastic-plastic material. A comparison with experiments shows that only the simulation with elastic-viscoplastic material behavior agrees very well with the measurements.

Figure 9 shows the effective plastic strain-rate along the axis of the steel rod close to the impact point where the plastic deformation is concentrated. In this case, the maximal effective plastic strain is 2.9% and plastic strain-rates of up to 1300 l/s are computed from the elastic-viscoplastic simulation. While both values are smaller than in the comparable aluminum simulation, their effects on the impact are significant. This is due to the strong increase of the yield stress with the strain-rate as identified from the material tests shown in Fig. 3.

In the following, the impact on the steel rod is analyzed at lower initial velocities. In Fig. 10, the sphere velocity and impact force are presented for a low velocity of v_0=0.32 m/s. Similar to the previously presented higher velocity the simulation with elastic-viscoplastic material behavior agrees best with the measurements. Again, these elastic-viscoplastic simulation results lie

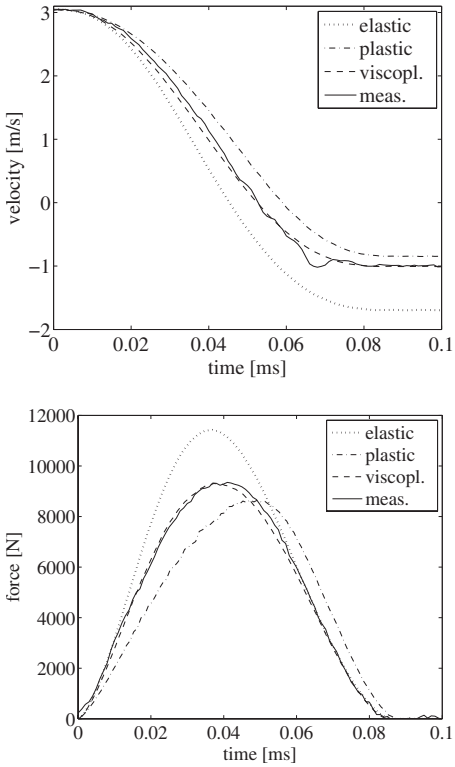

Fig. 8 Sphere velocity and impact force for impact with v_0=3.05 m/s on the steel rod

between the elastic and elastic-plastic simulation results, showing the influence of strain-rate effects also for lower velocities.

For the impact with v_0=0.32 m/s the effective plastic strain-rate at points along the axis of the steel rod close to the impact point are shown in Fig. 11. Note that for this lower velocity, the region of plastic deformation is much smaller than at the higher velocity. In this case, the last investigated point *h* is located 0.554 mm away from the initial point of impact. The maximal effective plastic strain computed from the elastic-viscoplastic simulation is here 0.84% and the maximal plastic strain-rate is about 250 l/s. Despite these relatively low strain-rates the elastic-viscoplastic material behavior has a significant influence as previously seen. This is due to the fact that the steel specimens show a very strong increase of the yield stress with small strain-rates, see Fig. 3.

Thus, the analysis of the results for impacts on the steel rod with v_0=0.32 m/s and v_0=3.05 m/s show that there is a significant influence of strain-rate effects on the impact and, therefore,

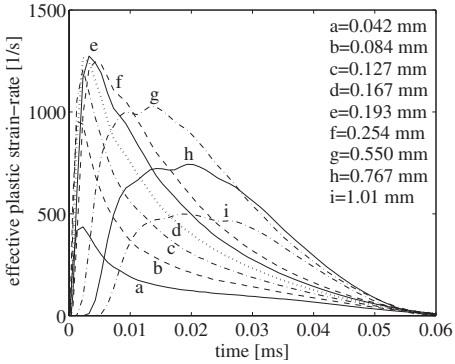

Fig. 9 Effective plastic strain-rate along the axis of the steel rod for impact with v_0=3.05 m/s

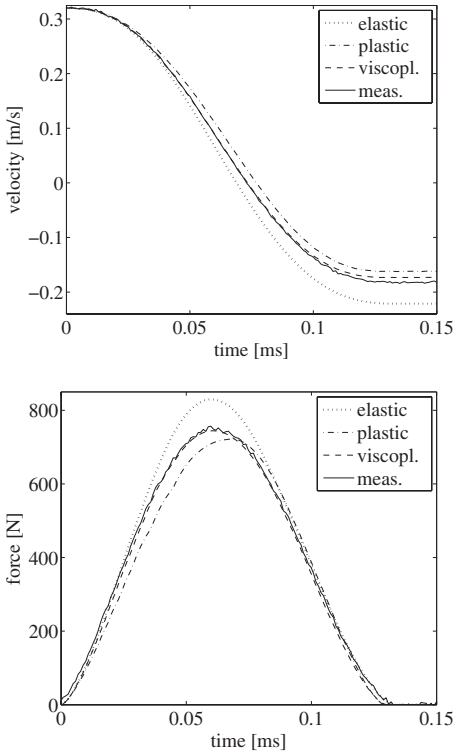

Fig. 10 Sphere velocity and impact force for impact with v_0=0.32 m/s on the steel rod

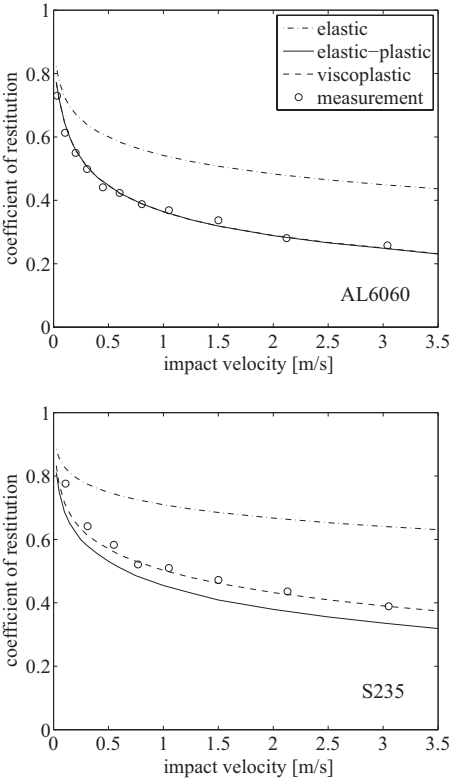

Fig. 12 Coefficient of restitution for impacts on aluminum and steel rod

the use of an elastic-viscoplastic material model is necessary. Only these simulations yield a correct impact behavior, whereas simulations with elastic material behavior overestimate the rebound velocity of the sphere, and simulations with elastic-plastic material behavior underestimate the rebound velocity of the sphere.

6 Coefficient of Restitution

The coefficient of restitution describes the macromechanical impact behavior. It summarizes the various sources of kinetic energy loss of the rigid body motion during impact, which in this study are the plastic deformations of the contact region and initiation of wave propagation in the rod. The sphere is a compact body and does not show any wave phenomena. Figure 12 shows the measured and simulated coefficients of restitution for both impact systems for the velocity range of 0.05–3.5 m/s. In all cases the decrease of the coefficient of restitution with increasing initial velocity is clearly seen. The simulations with elastic material yield the highest values. However, despite the absence of plastic deformation these values are well below 1. This is due to the transformation of a significant amount of kinetic energy from the rigid body motion into wave propagation. The detailed analysis of the influence of wave propagation and elastodynamic vibration in impacts on bodies with various shapes is given in Refs. [2,14].

The inclusion of plasticity results in additional kinetic energy loss of the rigid body motion, and thus in a further drop of the coefficient of restitution. For the impacts on the aluminum rods the coefficients computed from elastic-plastic and elastic-viscoplastic simulations are basically identical. In the entire velocity range these computed values agree very well with experimental values. This confirms the previous results that viscoplastic effects are negligible for impacts on the aluminum.

In contrast, for steel the coefficient of restitution computed from simulations using elastic-plastic and elastic-viscoplastic material behavior differ significantly. The results from elastic-viscoplastic simulations are notably higher than the ones from elastic-plastic simulations, which indicate smaller inelastic deformation due to the increase of yield stress with the strain-rate. It should be noted that this effect is even stronger in the absence of wave effects as demonstrated for the impact of two identical spheres in Ref. [15]. For the investigated rod a substantial amount of strain-energy is transformed into wave propagation, which reduces the impact force and thus the amount of inelastic deformation near the contact point. In contrast in the absence of wave effects higher impact force and more inelastic deformation can occur. Detailed analysis of the influence of wave propagation on impact processes are given for elastic and elastic-plastic material in Refs. [2,3,14]. For the steel specimen the coefficients of restitution evaluated from the elastic-viscoplastic simulations agree very well with the measured coefficients, whereas the elastic-plastic simulations underestimate the coefficient of restitution and the elastic simulations overestimate the coefficient of restitution.

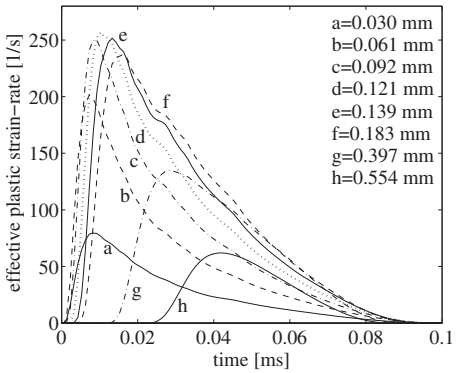

Fig. 11 Effective plastic strain-rate along the axis of the steel rod for impact with v_0=0.32 m/s

Again, this confirms that viscoplastic effects are significant for impacts on the steel and have to be included in numerical simulations.

7 Summary and Conclusion

In this research, the influence of viscoplastic effects of aluminum and steel on the impact process and the consequences for the coefficient of restitution are investigated. Thereby, aluminum AL6060 and steel S235 are used, and their static and dynamic material behavior is identified from quasi-static compression tests and dynamic split Hopkinson pressure bar tests. From these material tests Perzyna-like elastic-viscoplastic material models are identified, which show weak viscoplastic effects for the aluminum specimen and strong viscoplastic effects for the steel specimen. As an impact system, the longitudinal impacts of a hardened steel sphere on long aluminum and steel rods are analyzed numerically and experimentally in the velocity range of 0.05–3.5 m/s. These investigations show that in the entire velocity range viscoplastic effects are negligible for impacts on the aluminum rod. Therefore, FE simulations using an elastic-plastic material model are sufficient for its numerical impact analysis and yield very accurate results. In contrast, the analysis of steel shows significant viscoplastic effects during impact, which have to be included in the FE simulation in order to accurately evaluate the impact. Comparisons with measurements show that from the elastic-plastic FE simulation of aluminum and from the elastic-viscoplastic FE simulation of steel the coefficient of restitution can be evaluated very accurately for both impact systems. Thus, such FE simulations provide an efficient and accurate tool for the evaluation of the coefficient of restitution and they can be used to limit the amount of costly impact experiments for more general impact systems.

References

[1] Christoforou, A. P., and Yigit, A. S., 1998, "Effect of Flexibility on Low Velocity Impact Response," J. Sound Vib., **217**(3), pp. 563–578.
[2] Schiehlen, W., and Seifried, R., 2004, "Three Approaches for Elastodynamic Contact in Multibody Systems," Multibody Syst. Dyn., **12**, pp. 1–16.
[3] Schiehlen, W., Seifried, R., and Eberhard, P., 2006, "Elastoplastic Phenomena in Multibody Impact Dynamics," Comput. Methods Appl. Mech. Eng., **195**, pp. 6874–6890.
[4] Stronge, W. J., 2000, *Impact Mechanics*, Cambridge University Press, Cambridge.
[5] Lankarani, H. M., and Nikravesh, P., 1994, "Continuous Contact Force Models for Impact Analysis in Multibody Systems," Nonlinear Dyn., **5**, pp. 193–207.
[6] Glocker, C., 2001, "On Frictionless Impact Models in Rigid-Body Systems," Philos. Trans. R. Soc. London, Ser. A, **359**, pp. 2385–2404.
[7] Goldsmith, W., 1960, *Impact: The Theory and Physical Behaviour of Colliding Solids*, Edward Arnold, London.
[8] Sondergaard, R., Chaney, K., and Brennen, C. E., 1990, "Measurements of Solid Spheres Bouncing off Flat Plates," ASME J. Appl. Mech., **57**, pp. 694–699.
[9] Stoianovici, D., and Hurmuzlu, Y., 1996, "A Critical Study of the Applicability of Rigid-Body Collison Theory," ASME J. Appl. Mech., **63**, pp. 307–316.
[10] Wu, C.-Y., Li, L.-Y., and Thornton, C., 2003, "Rebound Behavior of Spheres for Plastic Impacts," Int. J. Impact Eng., **28**, pp. 929–946.
[11] Zhang, X., and Vu-Quoc, L., 2002, "Modeling the Dependence of the Coefficient of Restitution on the Impact Velocity in Elasto-Plastic Collisions," Int. J. Impact Eng., **27**, pp. 317–341.
[12] Seifried, R., Schiehlen, W., and Eberhard, P., 2005, "Numerical and Experimental Evaluation of the Coefficient of Restitution for Repeated Impacts," Int. J. Impact Eng., **32**, pp. 508–524.
[13] Jones, N., 1997, *Structural Impact*, Cambridge University Press, Cambridge.
[14] Seifried, R., 2007, "Effect of Body Flexibility on Impacts Studied on Rods and Beams," ASME Paper No. DETC2007-34817.
[15] Minamoto, H., and Kawamura, S., 2009, "Effects of Material Strain Rate Sensitivity in Low Speed Impact Between Two Identical Spheres," Int. J. Impact Eng., **36**(5), pp. 680–686.
[16] Minamoto, H., Seifried, R., Eberhard, P., and Kawamura, S., 2008, "Effects of Strain Rate Dependency of Material Properties in Low Velocity Impact," Int. J. Mod. Phys. B, **22**(9–11), pp. 1165–1170.
[17] Field, J. E., Walley, S. M., Proud, W. G., Goldrein, H. T., and Siviour, C. R., 2004, "Review of Experimental Techniques for High Rate Deformation and Shock Studies," Int. J. Impact Eng., **30**, pp. 725–775.
[18] Gama, B. A., Lopatnikov, S. L., and Gillespie, J. W., 2004, "Hopkinson Bar Experiment Technique: A Critical Review," Appl. Mech. Rev., **57**(4), pp. 223–250.
[19] Perzyna, P., 1966, "Fundamental Problems in Viscoplasticity," Adv. Appl. Mech., **9**, pp. 243–377.
[20] Simo, J. C., and Hughes, T. J. R., 1998, *Computational Inelasticity*, Springer, New York.
[21] Bathe, K. J., 1996, *Finite Element Procedures*, Prentice-Hall, Upper Saddle River, NJ.
[22] Zienkiewicz, O. C., and Taylor, J. Z., 2006, *The Finite Element Method for Solid and Structural Mechanics*, Elsevier, Amsterdam.
[23] Ansys, 2007, ANSYS Theory Reference, Release 11.0, Ansys Inc.
[24] Kikuchi, N., and Oden, J., 1989, *Contact Problems in Elasticity: A Study of Variational Inequalities and Finite Element Methods*, SIAM, Philadelphia.
[25] Wriggers, P., 2002, *Computational Contact Mechanics*, Wiley, Chichester.
[26] Zhong, Z.-H., 1993, *Finite Element Procedures for Contact Problems*, Oxford University Press, New York.
[27] Seifried, R., Hu, B., and Eberhard, P., 2003, "Numerical and Experimental Investigation of Radial Impacts on a Half-Circular Plate," Multibody Syst. Dyn., **9**, pp. 265–281.
[28] Polytec, 1994, Vibrometer's Manual for Polytec Vibrometer Series OFV-3000/OFV-302, OFV501 and OFV502. Manual No. VIB-MAN-9308-e04/01, Polytec, Waldbronn.
[29] Cunningham, D. M., and Goldsmith, W., 1958, "Short-Time Impulses Produced by Longitudinal Impact," Proc. Soc. Exp. Stress Anal., **16**(2), pp. 153–162.
[30] Graff, K. F., 1991, *Wave Motion in Elastic Solids*, Dover, New York.